Geol. Mag. **147** (3), 2010, pp. 321–338. © Cambridge University Press 2009
doi:10.1017/S001675680999046X

Palaeogene alluvial–volcaniclastic deposits in the Mesta Basin (SW Bulgaria): depositional setting and basin evolution

ANDREAS SIEMES*, TOM McCANN & ANNE FISCHER

Steinmann Institut, Universität Bonn, Nußallee 8, 53115 Bonn, Germany

(*Received* 16 June 2009; *accepted* 7 July 2009; First published online 27 October 2009)

Abstract – The Mesta half-graben is one in a series of extensional basins in SW Bulgaria that record the onset of extension within the Rhodope Zone in the Late Eocene. Tectonic activity on a continuous detachment along the eastern margin was a major control on subsidence, accommodation space creation, sediment supply and facies distribution in the basin. The sedimentary architecture was complicated by synsedimentary rotation, the presence of intrabasinal faults and the resulting compartmentalization, as well as synsedimentary volcanic activity. Facies and structural analysis of a key transverse section in the central part of the basin, together with supporting observations from other parts of the basin, indicate a pulsed tectono-sedimentary evolution of the basin with three distinct stages. The first stage (Late Eocene) is a phase of rapid extension with an initial alluvial setting. Basin margin fans and an axial fluvial through-drainage system were the major depositional systems in this stage. The second stage (Early Oligocene) marks the onset of volcanic activity within the Mesta Basin and is characterized by the formation of volcanic centres, an intense phase of explosive volcanism and rapid infilling of the previous basin topography with volcanic material deposited from pyroclastic density currents. The third stage (Late Oligocene) represents waning volcanic activity in a mixed alluvial–volcaniclastic environment. This stage is characterized by alternating alluvial and volcaniclastic depositional cycles, as well as partial reworking of volcanic material.

Keywords: alluvial, volcaniclastic, half-graben, detachment fault, Aegean extension, southwest Bulgaria.

1. Introduction

The timing and onset of Cenozoic extension within the Rhodope (Fig. 1) and the broader Aegean region is controversial. Several structural studies have suggested that Cenozoic extension in the Rhodope region was related to the formation of detachment faults and metamorphic core complexes (e.g. Dinter, 1998; Ricou *et al.* 1998, 2000; Bonev, Burg & Ivanov, 2006). Zagorchev (1998, 2000) attempted to refute the concept of a 'Rhodope metamorphic core complex', and Westaway (2006) also rejected any pre-Miocene extension in SW Bulgaria. However, recent structural studies have confirmed that Eocene to Early Oligocene large-scale normal faulting occurred in the Rhodope region (e.g. Tueckmantel *et al.* 2008; Bonev, Burg & Ivanov, 2006; Burchfiel *et al.* 2000, 2008). This phase of extension in the Rhodope region from the Late Eocene onwards resulted in the development of a series of related basins (Burchfiel, Nakov & Tzankov, 2003; e.g. Mesta, Padesh and Strymon basins; Fig. 1).

The Mesta Basin in SW Bulgaria is located in the southwestern part of the Rhodope region (Fig. 1). Previous studies have suggested a half-graben structure for the basin with a single continuous detachment fault bounding the basin in the east (Burchfiel, Nakov & Tzankov, 2003). The basin fill of more than 2500 m comprises alluvial, volcaniclastic and volcanic units, which provide a record of the onset of large-scale normal faulting in the area and allow the related tectono-magmatic-sedimentary evolution to be reconstructed.

This paper presents the first results from an ongoing study in the Mesta Basin and is part of a broader research project that addresses the tectono-sedimentary evolution of the Rhodope Zone. The aims of this paper are (1) to refine the facies environment and depositional setting of the basin infill and (2) to develop a preliminary model for the evolution of the basin. The stratigraphic relationships between the various units in the Mesta Basin have been previously studied (e.g. Burchfiel, Nakov & Tzankov, 2003; Harkovska, 1983; Zagorchev, 1998). Published geological maps of the area, however, differ considerably (Burchfiel, Nakov & Tzankov, 2003, pp. 63, 67; Harkovska, 1983, pp. 6, 7; Zagorchev, 1998, p. 104), and the precise stratigraphic framework is controversial (Burchfiel, Nakov & Tzankov, 2003).

We examined a key transverse section in the central part of the basin (Filipovo–Osenovo, Fig. 2), which is representative of the total infill of the central Mesta Basin. This key section records a continuous sedimentary succession of the Palaeogene basin fill. The clearly observed superpositional relationships between the various units in the section allow for an unbiased (with regard to the stratigraphy) interpretation of the evolution of the depositional environment within the central part of the basin, without having to consider

*Author for correspondence: andreas.siemes@gmail.com

Figure 1. Overview map of SW Bulgaria and adjacent regions. The locations of the Mesta, Padesh and Struma basins are highlighted in dark grey, and the locations of Figures 2 and 3a are shown in black. The approximate extent of the Rhodope Mountains is shown with a dashed line (modified after Burchfiel, Nakov & Tzankov, 2003).

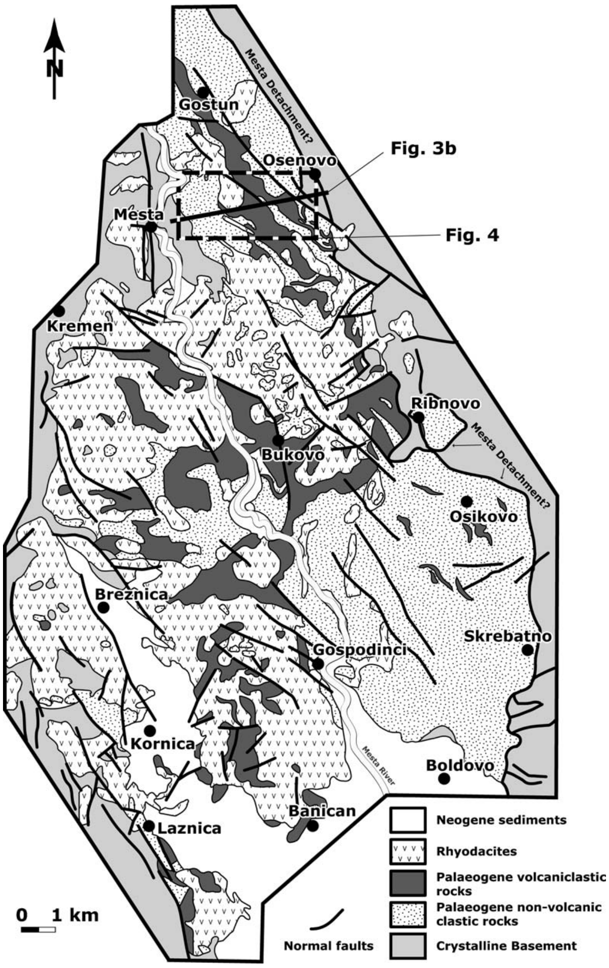

Figure 2. Geological map of the central part of the Mesta Basin (simplified after Harkovska, 1983). The locations of Figure 3b and the Filipovo–Osenovo map (Fig. 4) are shown.

the inherent problems of the previously published stratigraphic framework and any problematic lateral variations. However, the interpretations are limited to the central part of the basin, but do provide the groundwork for ongoing work in the basin. We do not discard the previous stratigraphy, but instead provide a short summary of the previous framework (see Section 3) and explain our reservations regarding its applicability (see Section 3.a).

The presence of a basin-bounding detachment fault together with a mixed alluvial–volcanic depositional system makes the Mesta Basin analogous for other detachment basins in extensional settings (e.g. Basin and Range Province, SW USA). The Mesta Basin is particularly interesting because of the preservation of several continuous basin fill successions, which allow the response to the onset of active volcanism within an alluvial half-graben setting to be reconstructed in detail.

2. Geological setting

The N–S-oriented Mesta Basin forms a trough-shaped depression along the Mesta River between the high-grade metamorphic and plutonic rocks of the Pirin and Western Rhodope mountains (Fig. 2). The basin contains a continental succession of Late Eocene to Oligocene sediments comprising conglomerates, breccias and sandstones interbedded with volcaniclastic and felsic volcanic rocks. The overall thickness varies from several hundred metres to more than 2500 m. The depositional environment is interpreted as mainly alluvial. The Palaeogene sediments rest unconformably on an uneven metamorphic basement surface and are overlain by Neogene alluvial sediments (Burchfiel, Nakov & Tzankov, 2003; Harkovska, 1983).

Basin initiation began in the Late Eocene and was coeval with the onset of Aegean extension in SW Bulgaria (Burchfiel, Nakov & Tzankov, 2003). The precise mechanisms of basin formation and subsidence are still unclear. The periods of extension could be related to activity at the Hellenic subduction zone or possibly to local rotation or shortening as a result of plutonic intrusions in the Rhodope Zone. Relative to the WNW orientation of Late Palaeogene magmatic intrusions in the region, the Mesta Basin and other Late Palaeogene extensional basins of SW Bulgaria show an oblique trend. Burchfiel, Nakov & Tzankov (2003) concluded that the regional syn-magmatic extension in SW Bulgaria was not perpendicular to the magmatic arc, and thus it is polygenetic. They further suggested that extension could be related to gravitationally induced lateral spreading within a thickened hot arc crust. This, combined with the fact that the arc shows pronounced variations in its thickness along strike, may have resulted in the development of a non-perpendicular orientation of the extensional structures relative to the arc (Burchfiel, Nakov & Tzankov, 2003). Another possibility is that slab rollback within the subduction system in the Hellenides resulted in periods of extension (Burchfiel, Nakov & Tzankov, 2003).

The Mesta Basin has been interpreted as a graben with N–S-striking normal fault systems forming the basin-bounding faults (Harkovska, 1983; Pecskay, Harkovska & Hadjiev, 2000). As noted above, more recent structural mapping (Burchfiel, Nakov & Tzankov, 2003) suggested a structure with a single listric detachment fault bounding the basin in the east (Fig. 3). This interpretation is mainly based on the fact that the dip of

https://doi.org/10.1017/S001675680999046X Published online by Cambridge University Press

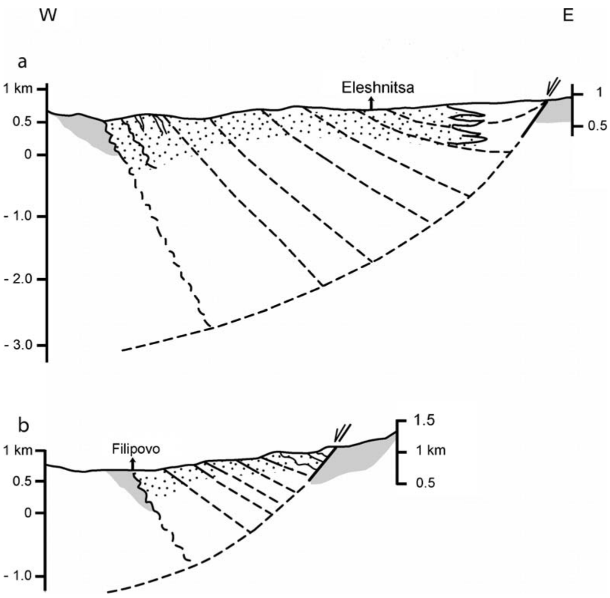

Figure 3. Cross-sections (ENE-trending) of the Palaeogene successions at Eleshnitsa (a – located about 13 km NW from Osenovo, location shown in Fig. 1) and Filipovo (b – location shown in Fig. 2); vertical and horizontal scales are equal (after Burchfiel, Nakov & Tzankov, 2003).

the basal sediments of the Palaeogene infill is 50–60° E and then changes to progressively lower angles towards the top of the sedimentary succession, suggesting a degree of synrotational deposition (Burchfiel, Nakov & Tzankov, 2003).

Geochronological data on subvolcanic intrusions and volcanic clasts in the Mesta Basin indicate a period of volcanic activity between 33 and 28 Ma (Pecskay, Harkovska & Hadjiev, 2000). Volcanic activity was mainly characterized by phreatomagmatic eruptions, subvolcanic intrusions and rarer extrusive eruptions. The main volcanic features in the Mesta Basin are a network of dome- or ridge-shaped subvolcanic bodies in the southern part of the basin and ubiquitous interbedded volcaniclastic sediments in the upper half of the basin infill. Two concentric volcanic structures near the villages of Banichan and Kremen are interpreted as the remnants of two calderas, which formed the main eruption centres in the basin (Harkovska, 1983). In addition, a series of linearly arranged volcanic intrusions constitute two volcano-tectonic zones (Gostun and Dobrinishte zones) and are probably related to intrabasinal faults (Harkovska, 1983). Harkovska *et al.* (1998) subdivided the volcanic rocks in the Mesta Basin into a younger and an older suite. The earlier volcanic phase (Late Priabonian–Early Rupelian) comprised explosive and phreatomagmatic eruptions with associated rhyodacitic rocks and coeval dacitic intrusions. The calderas probably formed towards the end of this phase (Harkovska *et al.* 1998). In the younger phase (Late Rupelian), explosive volcanic activity subsided and dacitic to rhyodacitic lava was extruded, while magma was intruded in the calderas and along the fault zones (Harkovska *et al.* 1998).

Volcanic features similar to the calderas and subvolcanic intrusions in the Mesta Basin are also known from the eastern Rhodope area, for example, the Sheinovet (Ivanova, 2005) and Borovitsa/Murga/Dushka calderas (Dhont *et al.* 2008). These calderas also formed during phases of acidic volcanism (trachyrhyodacitic to rhyolitic) in the Early Oligocene (34–30 Ma; Dhont *et al.* 2008), accompanied by the intrusion of high-K rhyolite domes, dykes and subvolcanic rhyodacite bodies (32 Ma; Ivanova, 2005). In both cases, pyroclastic current and fall deposits with magmatic and accidental lithic clasts and accretionary lapilli are abundant. Thus, it is likely that the Early Oligocene volcanic activity in the Mesta Basin was coeval with the formation of similar volcanic centres throughout the southern Rhodope region.

3. Stratigraphy

As noted in the previous Section, the more than 2500 m thick basin fill of the Mesta Basin consists mainly of Palaeogene-age alluvial coarse-grained clastic and fine- to coarse-grained volcaniclastic sediments that were intruded by felsic volcanic rocks. Stratification, where present, is frequently cut by local unconformities and intrabasinal faults.

Five Palaeogene-age lithostratigraphic formations have been recognized in the Mesta Basin (Harkovska, 1983): Dobrinishka Formation; Gradinishka Formation; Osikovo Formation; Zlataritsa Formation and Mesta Formation. Harkovska (1983) and Burchfiel, Nakov & Tzankov (2003) agree that most of the formations, except for the locally restricted Dobrinishka Formation, interdigitate laterally, resulting in complex stratigraphic relationships. For mapping purposes and structural interpretation, however, Burchfiel, Nakov & Tzankov (2003) assumed predominant overlying relationships between the four formations from the oldest (Dobrinishka) to the youngest (Zlataritsa) (see Fig. 3), although the precise spatial relationships are still subject to debate (see next Section). The main distinguishing criteria between the non-volcanic formations include a combination of clast composition, colour and facies associations.

The Dobrinishka Formation occurs only in the northwestern part of the Mesta Basin and comprises about 42 m of sandstones and conglomerates. The strata dip 70–80° E. Palynological data indicate a Late Eocene age (Ivanov & Chernyavska, 1972). The pollen data, however, are controversial (Zagorchev, 1998). Due to its limited occurrence, this formation has not been recognized as a mappable unit in past studies (Harkovska, 1983; Burchfiel, Nakov & Tzankov, 2003).

The Gradinishka Formation unconformably overlies the Dobrinishka Formation and metamorphic basement in other parts of the Mesta Basin. Controversial palynological dating also suggests a Late Eocene depositional age for this formation (Ivanov & Chernyavska, 1972). The formation thickness ranges from tens of metres to more than 700 m, according to Harkovska (1983),

https://doi.org/10.1017/S001675680999046X Published online by Cambridge University Press

and from several hundred to more than 1000 m, according to Burchfiel, Nakov & Tzankov (2003). The formation comprises grey to red polymictic breccia-conglomerates and conglomerates with lenses of finer-grained material (conglomeratic sandstones, sandstones and siltstones) (Harkovska, 1983).

The Osikovo Formation unconformably overlies the Gradinishka Formation. Regionally, the upper part of the formation directly overlies basement. The thickness of the formation varies from 0 to tens of metres to 900 m, according to Harkovska (1983), while Burchfiel, Nakov & Tzankov (2003) estimated it as locally up to 1000 m thick and laterally very variable. Harkovska (1983) subdivided the Osikovo into two stratigraphic members: conglomerates and breccia-conglomerates (Skok Member) and sandstones with associated siltstones and sandy conglomerates (Kupen Member). Gradual transitions between sandstone and conglomerate beds occur. The associated siltstones, locally muddy, are grey and contain dispersed organic matter with occasional plant detritus (Harkovska, 1983).

The Zlataritsa Formation only occurs in the northern part of the Mesta Basin and comprises the top of the Palaeogene infill. It overlies the Gradinishka and Osikovo formations and also laterally interdigitates with the upper part of the Osikovo Formation. Burchfiel, Nakov & Tzankov (2003) described the thickness of the formation as greater than 500 m. Harkovska (1983) estimated the thickness of the Zlataritsa Formation at between 0 to 500 m. The lithology of the Zlataritsa Formation is comparable to that of the Gradinishka Formation and comprises grey to greenish or reddish, weak- to medium-sorted polymictic breccia conglomerates, interbedded with very coarse sandstones (Harkovska, 1983).

The Mesta Formation comprises all of the volcaniclastic rocks of the Mesta Basin including tuffs, tuff-breccias, agglomerates, tuffaceous sandstones and conglomerates and epiclastic rocks of variable appearance. The composition of the volcanic components is acidic (dacite–trachydacite and rhyodacite: Pecskay, Harkovska & Hadjiev, 2000). Burchfiel, Nakov & Tzankov (2003) did not consider the volcaniclastic rocks as a distinct mappable unit and instead included them within the non-volcanic formations. The thickness of the Mesta Formation varies from 0 to 1200 m and decreases away from the volcanic centres in the southern part of the Mesta Basin (Harkovska, 1983).

3.a. Discussion

A lithostratigraphic formation should be defined according to the detail which is necessary for geological mapping in an area (Salvador, 1994). As noted above, a comparison of published geological maps of the Mesta Basin by Harkovska (1983, pp. 6, 7), Burchfiel, Nakov & Tzankov (2003, pp. 63, 67) and Zagorchev (1998, p. 104), as well as our own field observations (Fig. 4), reveal that the various mapped units are not easily

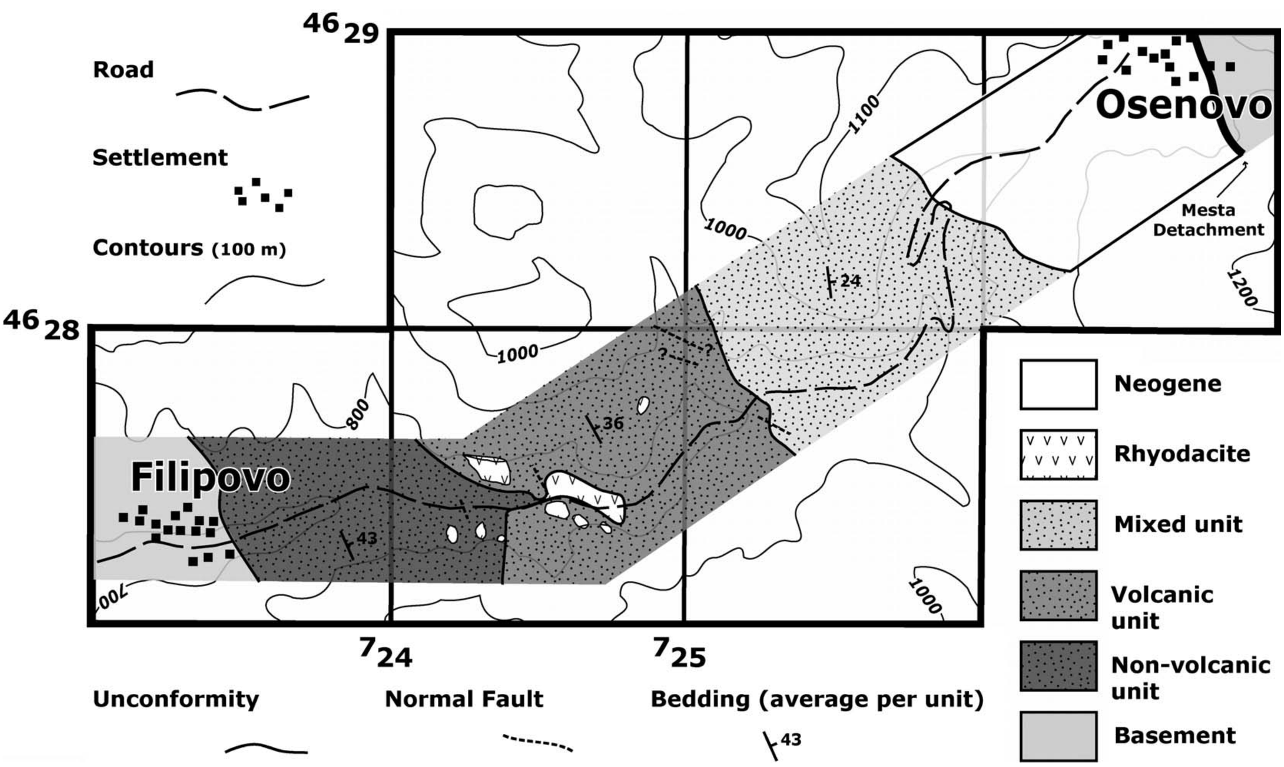

Figure 4. Geological map of the Filipovo–Osenovo section, illustrating the spatial relationships of the three depositional units (non-volcanic, volcanic, mixed). The lateral unit boundaries are not geological boundaries and only indicate the lateral extent of our field observations. The plotted strike and dip values (bedding) represent an average of all measurements per depositional unit (see Fig. 7). The coordinate grid is UTM (European 1955, due to the available topographic base map). Location shown in Figure 2.

https://doi.org/10.1017/S001675680999046X Published online by Cambridge University Press

correlatable and that there appear to be significant problems in accurately identifying individual stratigraphic units in the Mesta Basin. Thus, any correlation of these units on a basinwide scale is problematic. In addition, previous thickness estimates of the various formations also vary greatly, sometimes by as much as several hundred metres (see previous Section), thus contributing to the correlation problem. Therefore, we suggest that the stratigraphic framework for the Mesta Basin requires adjustments and refinement in order to reflect accurately the complexities of the depositional architecture within the basin (see Section 5). Below, we present a thorough reassessment of the depositional history of the central part of the Mesta Basin, which might serve as a basis for future stratigraphic work in the basin.

4. The Filipovo–Osenovo section

An approximately 2000 m thick continuous succession of Palaeogene sediments crops out along the Gradinishka River in the central part of the Mesta Basin (Figs 2, 4). The sediments are well exposed along road and river outcrops and extend from the village of Filipovo to the village of Osenovo. The sediments dip E to NE, and the E–W-oriented incised river valley allows a detailed analysis of the succession. Towards the west, the sedimentary succession unconformably overlies metamorphic basement rocks (gneiss). Towards the east, the Palaeogene sediments are unconformably overlain by loose, sandy conglomerates of Neogene age, while in the Osenovo area, the succession is bounded by the Mesta Detachment and metamorphic basement. Harkovska (1983) and Burchfiel, Nakov & Tzankov (2003) both mapped the occurrence of all of the major non-volcanic formations (Gradinishka, Osikovo and Zlataritsa) between the villages of Filipovo and Osenovo. Thus, the succession represents a key section for the infill of the Mesta Basin and an ideal case study to test the older stratigraphic scheme (Harkovska, 1983).

Three main facies associations occur throughout the succession (see Table 1 for facies codes and overview): non-volcanic clastic deposits (rudite facies association – RF), volcaniclastic deposits (volcaniclastic facies association – VCF) and intrusive subvolcanic acidic rocks (volcanic facies – VF). These three facies associations can be subdivided into several distinct subfacies. Based on facies architecture, the Filipovo–Osenovo can also be further differentiated into three depositional units (see Section 5). These units do not represent any of the previously described stratigraphic units, but rather record different stages in the evolution of the basin (see Section 6).

Table 1. Summary table of the occurring facies and subfacies in the Filipovo–Osenovo section

Facies associations		Characteristics	Interpretations
RF	*Rudite facies*		
RF1	Red/grey rudites	Sheets of massive crudely stratified, matrix-/clast-supported, red/grey pebble to boulder breccia-conglomerates with sandy matrix	Concentrated and hyperconcentrated sedimentary gravity flows with variable sediment-water ratios and grain size distributions
RF1S	Red/grey sandstones	Laterally confined fine to coarse grained sandstones and granule to pebbly sandstones, associated with RF1	Confined channel-fill deposits of small short-lived fluvial systems or winnowing of debris flow fines by streamflow
RF2	Marble breccias	Isolated interbeds of massive, matrix-supported, grey breccias with microcrystalline calcareous matrix and prevailing marble clasts	Isolated hyperconcentrated or debris sedimentary gravity flows related to slip events along the Mesta Detachment
RF3	Grey granite conglomerates	Sheets of massive, matrix-/clast-supported, monomictic granite conglomerates	Same as RF1 with different source material
VCF	*Volcaniclastic facies*		
VCF1	Thin-bedded volcaniclastics	Laminated to thin bedded, interbedded red/grey volcaniclastic sandstones to granule/pebbly volcaniclastic breccia-conglomerates	Pyroclastic surge deposits, turbulent flow dominant; distal facies or deposited during weaker eruption phases
VCF2	Thick-bedded volcaniclastics	Medium to thick bedded, interbedded red/grey volcaniclastic sandstones to granule/cobble volcaniclastic breccia-conglomerates	Pyroclastic flow deposits, turbulent and laminar flow component; more proximal facies or deposited during stronger eruption phases
VCF3	Massive volcaniclastics	Massive, chaotic red/grey volcaniclastic sandstones with floating pebbles to boulders and pebble to boulder breccia-conglomerates	Pyroclastic flow deposits, laminar flow dominant; even more proximal facies or deposited during even stronger eruptions phases
VCF4	Secondary volcaniclastic breccia	Massive, grey/green volcaniclastic breccia with partly altered volcanic clasts	Pyroclastic flow deposits (laminar) or hyperconcentrated sedimentary gravity flows of reworked pyroclastic material
VCF5	Lenticular volcaniclastics	Interbedded grey volcaniclastic sandstones and granule to pebbly conglomerates; stacked, lenticular beds	Stacked channel sequences, reworked pyroclastic material deposited in a fluvial environment
SVF	*Subvolcanic facies*		
SVF	Subvolcanic intrusions	Coarse- to fine-grained, porphyric rhyodacites	Dome- and ridge-shaped subvolcanic intrusions; magma emplacement probably controlled by intrabasinal faults

Unfortunately, palaeoflow indicators are very rare throughout the succession (see Section 4) and make it difficult to interpret palaeoflow directions and the palaeoenvironment.

4.a. Rudite facies association (RF)

The non-volcanic facies association (RF) comprises rudites with associated sandstones. The conglomerates and breccias differ in terms of sorting, grain-size distribution, composition, clast-support characteristics, clast fabric and stratification. The distinction into the different subfacies is mainly based on (a) variations in clast-support characteristics, (b) changes in clast and matrix composition and (c) differences in clast mode, size and shape. Four subfacies of non-volcanic sediments have been recognized in the Filipovo–Osenovo section: red to grey breccia-conglomerates (RF1), red to grey sandstones (RF1S), marble breccia (RF2) and grey granite conglomerates (RF3).

The red to grey breccia-conglomerates (RF1) are massive to crudely stratified, matrix- to clast-supported, poorly sorted and polymodal (Fig. 5a–c). They can be ungraded, inversely or normally graded. The dominant clast size ranges from pebble to boulder, with rare blocks up to several metres in diameter (max. 3.25 m, Fig. 5c). The clasts are sub-rounded to sub-angular. The composition is polymictic and varies between single beds. Approximately 40–80 % of the clasts are always granite to granodiorite. The other fraction consists of gneiss, marble, pegmatite, quartzite, amphibolite and serpentinite. The matrix consists of fine- to coarse-grained, red, reddish grey or grey quartz sand. Slight imbrication of clasts often occurs with the long axis of clasts oriented parallel to the bedding plane (E-dipping). The matrix–clast ratio ranges from 40:60 to 15:85. Bed thickness varies between rare medium to thick and very thick. However, thicker breccia-conglomerate units (tens to hundreds of metres thick) with internally indistinct bedding also occur. The bed geometry is often lenticular on a scale of several metres. Rarely, channel geometries can be observed (N–S orientation). Bed contacts are indistinct to sharp and mostly irregular and erosive. Soft sediment deformation features occur and are probably related to loading or impact structures of large boulders.

The red to grey associated sandstones (RF1S) are fine- to coarse-grained sandstones or granules to pebbles and sandstones. The sands are well sorted to immature, sometimes with floating pebbles and granules. The grains are rounded to subangular. The sand grains are dominantly quartz, feldspar and lithic fragments. The pebbles and granules consist of granite, milky quartz, gneiss and other metamorphic clasts. The composition is identical to that of the matrix of the RF1 rudites. Parallel and cross-lamination occur. Bed form is mainly lenticular and the sand layers occur as isolated bodies within the breccia-conglomerates. Sandy units in the succession are sometimes made up of several stacked lenticular sandstone layers.

The marble breccia (RF2) is a light to dark grey breccia that is massive, ungraded, matrix-supported and bimodal to polymodal. The breccia forms several isolated single beds within the larger RF1 succession. The dominant clast size ranges from pebble to cobble (although large boulders up to 2.40 m in diameter also occur). The clasts are angular to sub-rounded. The polymictic breccia is composed of light red to white marble and other metamorphic clasts (e.g. gneiss) and a microcrystalline calcareous grey matrix. The induration of the breccia is very hard. The breccia occurs as isolated very thick beds with a very irregular base. Bed geometry is lenticular to planar with sharp boundaries.

The grey granite conglomerates (RF3) are very similar to the red to grey breccia-conglomerates (RF1). The major differences are that the clasts are well-rounded to sub-rounded with only rare sub-angular clasts and that the composition is almost monomictic. The matrix consists of medium- to coarse-grained, light to dark grey sand.

4.a.1. Interpretation

The rudite facies association (RF) deposits cover a great variety of different breccia-conglomerates. Such coarse-grained sediments in a continental setting are usually the result of either bedload transport in a river system or sedimentary gravity flows in a high energy alluvial facies environment with steep gradients (cf. Collinson, Mountney & Thompson, 2006; Nemec & Steel, 1984). Massive beds, clast sizes up to several metres in diameter, as well as the bed form and the rare presence of interbedded sandstones, suggest that subaerial gravity flows of sediment–water mixtures were the major transport process responsible for the deposition of the rudites (cf. Blair & McPherson, 1994). Such sedimentary gravity flows are usually initiated on steep slopes. Common triggers include precipitation, tectonic activity and seasonal climatic fluctuations (Collinson, Mountney & Thompson, 2006; Malet *et al.* 2005). The flow type of sedimentary gravity currents is mainly determined by the ratio between the particulate sediment and the suspension medium (that is, gas or liquid). Dilute and less dense flows are more likely to show turbulent flow behaviour, while concentrated, dense flows are characterized by laminar flow (Waltham, 2004). The presence of different particle-support mechanisms, that is, both matrix- and clast-supported rudites, infers that various modes of transport occurred. The following interpretations are based on classification schemes for sedimentary gravity/density flows by Collinson, Mountney & Thompson (2006) and Mulder & Alexander (2001).

Matrix-supported rudites can either result (1) from cohesive debris flows with sufficiently high clay content or (2) from hyperconcentrated flows with highest grain concentrations (cf. Mulder & Alexander, 2001). In the former case, a sufficiently high clay content results in a matrix viscosity that acts as dominant

https://doi.org/10.1017/S001675680999046X Published online by Cambridge University Press

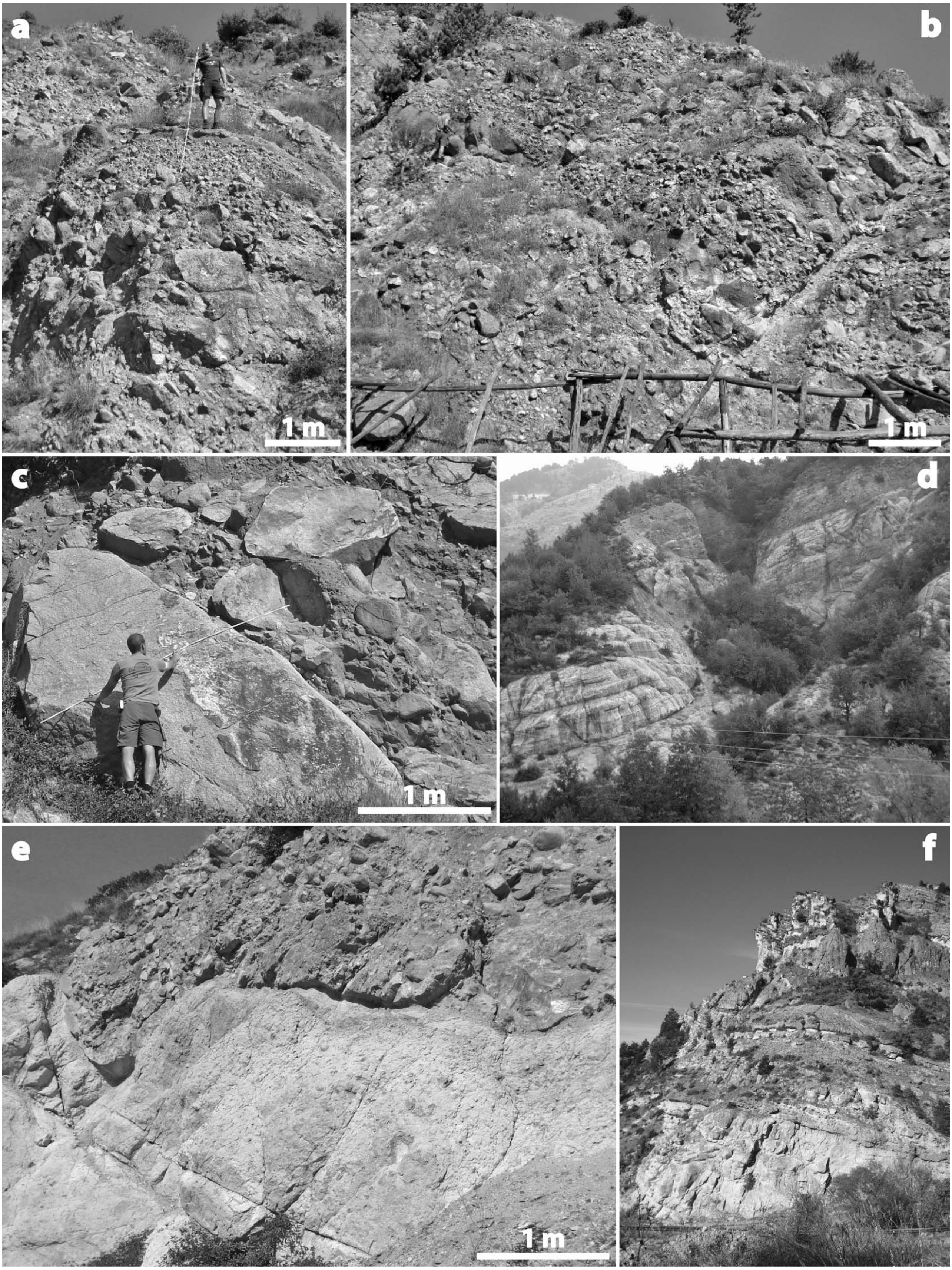

Figure 5. Field photos of (a) clast- and matrix-supported red breccia-conglomerates (RF1); (b) red breccia-conglomerates interbedded with associated sandstones (RF1S); (c) clast-supported red breccia (RF1) with large boulder; (d) non-volcanic rudites (RF1, upper right corner) overlying thin- to thick-bedded volcaniclastic rocks (VCF1–2); height of cliff is about 20 m; (e) non-volcanic rudites (RF1) overlying thick-bedded to massive volcaniclastic rocks (VCF2–3); (f) thick-bedded to massive volcaniclastic rocks (VCF2–3) interbedded with lenticular volcaniclastic rocks (VCF4) and non-volcanic rudites (RF1); height of cliff is about 150 m. (a, b, c) non-volcanic unit; (d) boundary between volcanic and mixed unit; (e, f) mixed unit. All photos were taken along the Filipovo–Osenovo road (see Fig. 4).

https://doi.org/10.1017/S001675680999046X Published online by Cambridge University Press

particle-support mechanism. In the latter case, intergranular collisions produce the matrix strength of the flow and support larger particles (Collinson, Mountney & Thompson, 2006; Mulder & Alexander, 2001; Coussot & Meunier, 1996). Most of the matrix-supported rudites of the Filipovo–Osenovo section show a low clay content and are, therefore, most likely the result of hyperconcentrated gravity flows.

Clast-supported rudites can form from concentrated (cf. Mulder & Alexander, 2001) and hyperconcentrated flows. Such flows are characterized by intergranular collisions or a turbulent flow component which both combine to sustain the flow. A higher concentration of particles relative to the water content and matrix increases the impact of intergranular collisions, while dilution results in more turbulence. The sedimentary characteristics of the resulting deposit depend upon which of the sustaining flow components was more dominant during the flow event. This, in turn, depends on the grain size distribution and sediment–water ratio (Collinson, Mountney & Thompson, 2006; Mulder & Alexander, 2001; Coussot & Meunier, 1996). The variable texture of the clast-supported rudites in the Filipovo–Osenovo section suggests that concentrated and hyperconcentrated flows with variable sediment–water concentration were predominant.

Most of the observed sedimentary structures within the present rudite beds can be explained by variable sediment–water ratios and different grain size distributions. Normal grading and sorting mostly occur in flows with a turbulent flow component, which allows vertical settling and sorting of particles. Thus, normal graded bedded layers are indicative of more dilute concentrated mass flows. In contrast, inversely graded beds develop due to a combination of dispersive pressure as a result of intergranular collisions and kinetic sieving. Therefore, inverse grading in rudite beds indicates higher concentrated or hyperconcentrated flow events. Flow transformations between laminar and turbulent flow may also occur (Felix & Peakall, 2006; Waltham, 2004) and might explain certain observed hybrid beds, which could not solely be the result of either laminar or turbulent flow.

The variable composition of the rudites most likely reflects the heterogeneity of the source area (see Section 5.a) or hints at several different source areas. The variable clast shapes from sub-angular to well-rounded suggest varying degrees of maturity and indicate that some sediments were subject to fluvial transport prior to being integrated into a sedimentary gravity flow.

The sandstones (RF1S) are always closely associated with the breccia-conglomerates and only occur as relatively thin, often lenticular, interbeds within the thicker non-volcanic successions. They may either be the deposits of smaller short-lived fluvial systems or of gravity flows in which the source material was previously sorted. Laterally confined channel-fill deposits may also be related to winnowing of debris flow fines by streamflow (cf. Blair & McPherson, 1992).

4.b. Volcaniclastic facies association (VCF)

This facies association comprises primary well-stratified thin- (VCF1) (Fig. 6d) to thick-bedded (VCF2) volcaniclastic rocks (Fig. 6c), massive volcaniclastic sandstones to breccias (VCF3), as well as secondary reworked volcaniclastic breccias (VCF4) and lenticular volcaniclastic rocks (VCF5). The major constituents of the volcaniclastic facies are sand-sized volcanic fragments, granule- to cobble-sized (rare boulders) magmatic lithic clasts (juvenile and accessory) and granule- to pebble-sized (rare cobbles) accidental clasts (granite and metamorphic). Most of the volcaniclastic rudites are matrix-supported breccias. The various facies types differ mainly in terms of their bedding and texture.

The thin-bedded volcaniclastic rocks (VCF1) consist of thin interbedded, often alternating, red and grey volcaniclastic sandstones or granule to pebbly volcaniclastic breccia-conglomerates (Fig. 6d). The sand layers are laminated to thin-bedded. Bed geometry is mostly parallel with planar, wavy, lenticular or irregular stratification. The clast size is mainly fine- to coarse-grained sand, with rare muddy or silty intervals. Constituent grains, up to sand size, are mainly volcanic material (predominant quartz, unidentifiable ash, biotite, feldspar, pumice and magmatic lithic clasts). Granules and pebbles mainly represent accidental lithic (granite, gneiss, serpentinite, marble) or magmatic lithic (white to grey volcanic) clasts (Fig. 6a). The latter are fine-grained holocrystalline rocks with variable alteration and a rhyodacitic composition (mainly quartz, feldspar, biotite). Round- to oval-shaped clasts (0.5–1.1 cm in diameter) with a brown/red or green/grey clay coating are concentrated in distinct layers. These aggregates consist of an assemblage of various sand-sized volcanic components that are surrounded by a thin clayey rim (Fig. 6b). They sometimes show a concentric internal structure of several rings of volcanic material, decreasing in grain size outwards, alternating with thin clay laminae. Granules and pebbles also occur as isolated matrix-supported layers or in the form of lenses with a clast-supporting fabric. Intervals with floating granules and pebbles also occur in the sandstone layers. The clasts are sub-rounded to angular. Low-angle cross-lamination is common in the fine- to medium-grained sand layers. Inverse and normal grading occur, the former being more common. The bed contacts are mostly sharp and erosive or gradual. Deformation structures occur in the form of low depressions and curved layer contacts around or beneath clasts.

The thick-bedded volcaniclastic rocks (VCF2) are medium to very thick (up to 3.5 m) interbedded, often alternating, red and grey volcaniclastic sandstones and granule to cobble breccia-conglomerates. Bed geometry is mostly parallel with planar or irregular stratification. Wedge-shaped cross-stratified beds rarely occur. The texture varies from medium- to coarse-grained sand (with floating granules to cobbles) to matrix-supported pebble and cobble breccia-conglomerates

https://doi.org/10.1017/S001675680999046X Published online by Cambridge University Press

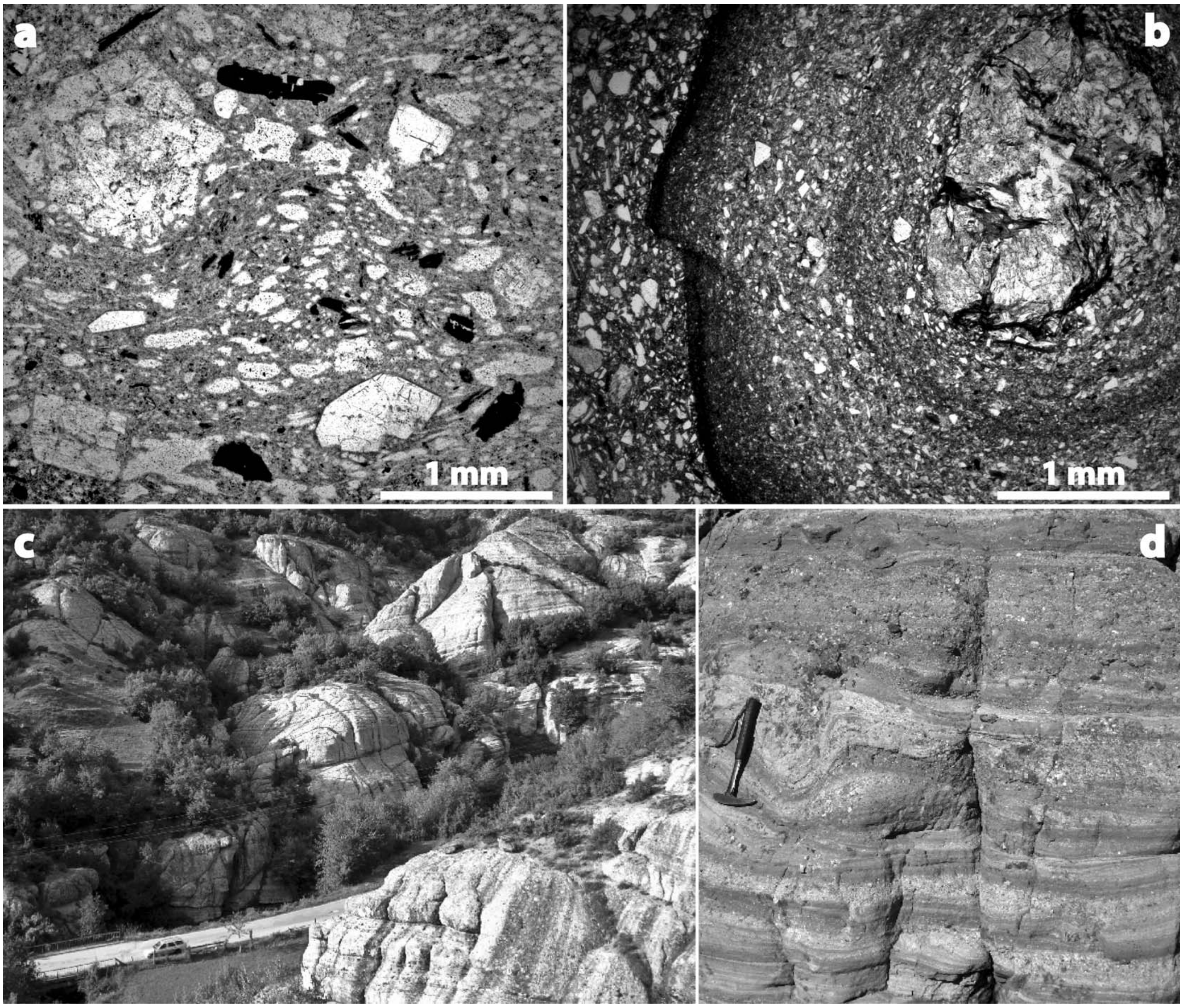

Figure 6. Thin-section photos of (a) a slightly welded ignimbrite within the VCF2 with dominantly quartz, feldspar and biotite crystals; (b) an accretionary lapilli within VCF1 including a crystal-fragment nucleus (feldspar/chlorite clast) coated with fine to coarse ash. Field photos of (c) alternating thin- to thick-bedded volcaniclastic rocks (VCF1–2) width of field of view is about 40 m, and (d) close-up of thin-bedded volcaniclastic rocks (VCF1) with bomb sag structure (next to hammer; hammer = 32 cm long). (c, d) volcanic unit; photos taken along the Filipovo–Osenovo road (see Fig. 4), about 1.7 km east from Filipovo.

and rarer clast-supported breccia-conglomerates. The clasts are angular to sub-rounded. The clast size ranges from granule to cobble (rare boulders). Clast composition is almost identical to the thin-bedded volcaniclastic facies (VCF1). The clasts are sometimes altered (baked), for example, some granite clasts are discoloured to a deep red. Within a single layer, the magmatic lithic clasts are mostly larger than the accidental clasts.

The massive red to grey volcaniclastic unit (VCF3), in contrast to the thin- and thick-bedded volcaniclastic facies (VCF1/2), shows no evidence of bedding. The internal structure is chaotic. Lithologically, the facies varies from medium- to coarse-grained volcanic sandstones with floating pebbles to boulders, to matrix-supported pebble to boulder breccia-conglomerates with rare clast-supported bands. The clasts are angular to sub-rounded. The composition is similar to the thin- and thick-bedded facies (VCF1/2) with variable ratios between magmatic lithic and accidental granite and metamorphic clasts. Bed contacts are indistinct to sharp and erosive.

One volcaniclastic breccia (VCF4) is remarkably different from the others and occurs as a single bed with a thickness of about 25 m. The breccia is grey-green and matrix-supported, with an internal chaotic structure and a monomictic composition. The matrix consists of coarse-grained sand (quartz, feldspar, biotite). The clasts are of rhyodacitic to dacitic composition, pebble to cobble sized (rare boulders) and partly altered. The fraction of clasts relative to the matrix is much higher in this unit than in the previous volcaniclastic facies (VCF1–3).

The lenticular volcaniclastic rocks (VCF5) are composed of interbedded units of grey fine- to coarse-grained sand, granular to pebbly conglomerates and rare muddy intervals. Grains (up to 2 mm in diameter) are mainly quartz, biotite and feldspar. The clasts are rhyodacitic volcanics, volcaniclastic fragments, quartz, granite (often altered) and metamorphic components. The conglomerates are usually matrix-supported. Sand layers often contain floating clasts of angular volcanics (up to pebble sized). Bed boundaries are sharp and erosive to gradual. The lenticular bed geometry and lateral thickness variations are characteristic for this facies. The lenticular beds sometimes occur as a series of stacked lenticular units. Parallel and cross-bedding occur within the lenticular layers. Coarsening- and fining-up sequences are abundant. Regular alternations between dark grey fine- to medium-grained sands and light grey coarse sands are also frequent. In one location, a 0.2 m thick unit of mottled reddish grey mud with a lateral extent of 2 m was observed. Similar isolated laminae of red mud occurred at the top of several sand layers.

4.b.1. Interpretation

The petrography of the sedimentary constituents within the volcaniclastic deposits suggests that they were derived from contemporaneous explosive volcanic eruptions. The observed bedding characteristics, sedimentary structures and compositional variations narrow the possible types of volcaniclastic sediments to pyroclastic flow or fall deposits. Abundant cross-lamination in the thin-bedded layers, chaotic textures in the massive beds, lenticular bed geometries and the confined lateral extent suggest that pyroclastic density currents (pyroclastic surges and flows: *sensu* Burgisser & Bergantz, 2002), that is, particle-laden, gravity-driven flows of volcanic origin (cf. Choux, Druitt & Thomas, 2004), were the dominant transport mechanism for the volcaniclastic material. The particle size of such currents can range from micrometric ashes to decimetric–metric blocks (Roche *et al.* 2005). The possibility that the volcaniclastic sediments were subsequently eroded and reworked following initial deposition (epiclastic sediments) cannot be ruled out for the thick-bedded to massive beds and is most likely the case for the altered volcaniclastic breccia (VCF4) and the lenticular volcaniclastic facies (VCF5).

As with sedimentary gravity flows, pyroclastic flows can be subdivided according to basic flow properties (Collinson, Mountney & Thompson, 2006; Waltham, 2004). The normal grading as result of vertical settling and sorting, as well as cross-lamination within certain layers (VCF1), suggests that turbulent flow occurred. However, more chaotic and structureless layers (VCF2, VCF3) with no grading or sorting, as well as floating clasts, are probably the result of laminar flow. Depositional characteristics typical for both flow types occur in the thin- to thick-bedded layers in close proximity to each other. This suggests that turbulent as well as laminar flow occurred in the same depositional environment. The turbulent flow deposits are probably related to dilute pyroclastic surges and the laminar flow deposits to denser ignimbrite flows (cf. McPhie, Doyle & Allen, 1993) or basal concentrated, granular flows (cf. Burgisser & Bergantz, 2002). The major difference between pyroclastic surges and ignimbrite flows is the sediment–water–gas concentration of the flow. In dense, granular flows, gas plays a subsidiary role, whereas gas in highly diluted, turbulent systems acts as the dominant transport mechanism (Lube *et al.* 2006). The concentration of a flow can change during the course of a flow; erosion and integration of more material can lead to a higher concentration of sediment, while deposition or water/gas entrainment can result in the dilution of the flow (Waltham, 2004; Felix & Peakall, 2006; Collinson, Mountney & Thompson, 2006). This may be an explanation for the rapid alternating successions and the close spatial associations for bed types originating from different types of flow.

Deformed beds and laminae are probably the result of impact marks (bomb sags: *sensu* Cas & Wright, 1987) of relatively isolated tephra fall-out from nearby explosive eruptions. However, other extraformational non-volcanic clasts with no associated deformation structures within the volcaniclastic facies were probably entrained or eroded by pyroclastic flows (= accidental clasts: McPhie, Doyle & Allen, 1993; Fisher & Schmincke, 1984).

The clay-rimmed concentric aggregates of volcanic material are accretionary lapilli. These spherical assemblages of volcanic grains form if a nucleus falls through a volcanic ash cloud and accumulates volcanic material around itself, and they are thus a strong indicator for explosive volcanism. They can flatten upon hitting the ground and can withstand a certain degree of further transport. They are often related to primary volcaniclastic deposits from phreatomagmatic eruptions (cf. McPhie, Doyle & Allen, 1993), in which they are usually abundant in fall deposits and occur more rarely in pyroclastic flow and surge deposits (Sparks *et al.* 1997). Most of the observed accretionary lapilli were intact and their occurrence was mostly limited to the thin-bedded volcaniclastic layers, which speaks for a relative low energy depositional environment for this facies type compared to the other ones.

Rapid alternating interbeds, cross-lamination, homogeneous grain-size distribution and grain sizes between fine sand and granule conglomerate all support the assertions that the thin-bedded volcaniclastic rocks (VCF1) were deposited by pyroclastic surges. The predominant thickness (millimetres to centimetres) indicates that it was a fairly distal facies because pyroclastic surges mostly only attain thicknesses of up to 1 m in direct proximity to the respective volcanic centres (cf. McPhie, Doyle & Allen, 1993).

The greater thicknesses of the thick-bedded and massive volcaniclastic facies (VCF2/3), as well as their chaotic internal structure and greater average grain size, suggests that these facies were deposited in a higher energy environment by denser laminar pyroclastic flows, that is, ignimbrite or lahar flows. It is likely that these facies represent a more proximal equivalent to the thin-bedded volcaniclastic facies (VCF1) relative to the volcanic centres or that they were deposited during periods of marked explosive activity.

The monomictic volcaniclastic breccia (VCF4) was also deposited in a high energy environment, either by a very dense pyroclastic flow or by a concentrated or hyperconcentrated sedimentary gravity flow. This breccia probably represents the first occurrence of secondary volcaniclastic sediments in the Filipovo–Osenovo section and its role will be further discussed in Sections 5.b and 5.c.

The lenticular volcaniclastic facies (VCF5) was most likely deposited in a fluvial environment and thus also represents secondary volcaniclastic deposits. The lenticular bed geometry and stacked channel sequences, which were not observed in the other volcaniclastic facies, support this assumption. The thin mud units could be related to weathering and soil horizons in abandoned fluvial channels or overbank areas.

4.c. Subvolcanic facies (VF)

The subvolcanic rocks present in the Filipovo–Osenovo section comprise coarse- to fine-grained rhyodacites. The texture is porphyric with a greyish white to black microcrystalline matrix (sometimes glass) and larger phenocrysts. The phenocrysts are mostly quartz (< 1.5 cm), plagioclase (< 2 cm), biotite (> 1 cm) and sanidine (rarely up to 12 cm long). The fine-grained mineral fraction consists of quartz, feldspar (plagioclase and K-feldspar/sanidine), biotite, amphibole, clinopyroxene and glass. Xenoliths include altered granites and metamorphic rocks.

The rhyodacite bodies form a series of dome- and ridge-shaped volcanic intrusions. These bodies may be isolated or occur as a semi-continuous ridge through the central part of the succession. In detail, the individual ridges consist of smaller disconnected segments of equal orientation (NW–SE). The contact zones between the intrusion bodies and the surrounding rocks are often altered or baked. The thickness of the subvolcanic bodies varies from several metres to tens of metres.

4.c.1. Interpretation

The rhyodacites of the Filipovo–Osenovo section may be related to the presence of a network of subvolcanic bodies located in the southern part of the Mesta Basin. The strike direction (NW–SE, 125–130°) of most of these rhyodacite bodies corresponds to the orientation of the Gostun linear volcano-tectonic zone as defined by Harkovska *et al.* (1998). Thus, the observed intrusions may be related to this volcanic structure and can be interpreted as possibly representing a series of intrabasinal faults controlling magma emplacement.

Pecskay, Harkovska & Hadjiev (2000) dated the K–Ar age of one of the intrusion bodies along the road between Filipovo and Osenovo (sample no. 281) at 30 ± 1.1 Ma (whole rock) and at 38.4 ± 1.5 Ma (plagioclase). The crystallization age of the plagioclase may represent a remnant of early crystallization within the magma chamber and the whole rock age could be closer to the actual emplacement age. However, the whole rock date may also be unreliable due to argon loss during weathering and more data are required to confirm the exact timing of volcanism within the Mesta Basin. Based on the spatial relationships between the rhyodacitic bodies and the surrounding sediments (e.g. baked contact zones), the subvolcanic bodies intruded subsequent to the deposition of the non-volcanic and volcaniclastic sediments.

5. Facies architecture and depositional setting

The various facies types can be grouped into three depositional successions, which represent the basal, middle and upper parts of the Palaeogene sediments between the villages of Filipovo and Osenovo (Fig. 4). The three units unconformably overlie one another from west to east and each contains a characteristic set of facies and architectural elements (Fig. 8). The units can be further distinguished and separated by sedimentary unconformities, intrabasinal faults and volcanic intrusion contact zones.

Comparison of all of the measured azimuth and dip orientations for all three units (Fig. 7) indicates that the dominant dip direction is N–NE and that, overall, the dip angle progressively decreases from the base to the top of the succession.

5.a. Non-volcanic unit

This unit comprises the basal part of the succession with a thickness of about 700 m, unconformably overlying metamorphic basement rocks near the eastern edge of the village of Filipovo. The unit is composed of sheets of massive to crudely stratified and graded breccia-conglomerates (RF1–3), as well as channel-fill breccia-conglomerates and interbedded sandstones (e.g. Fig. 8). The internal structure of the non-volcanic unit is variable. Medium- to very thick-bedded breccia-conglomerates with associated thin- to thick-bedded sandstones are interbedded with units that are indistinctly bedded and up to tens of metres thick. Nearly all of the observed beds are discontinuous over a scale of several metres. The dip direction of the breccia-conglomerates and sandstones in the non-volcanic unit varies between 354 and 058°. The dip ranges from 66 to 31° (Fig. 7a).

As noted in Section 4.a, the rudites were probably deposited by sedimentary gravity flows in a high-energy environment while the associated sandstones may be related to fluvial processes. Abundant large clast sizes indicate relatively short transport distances. However, the variable clast size and shape, including

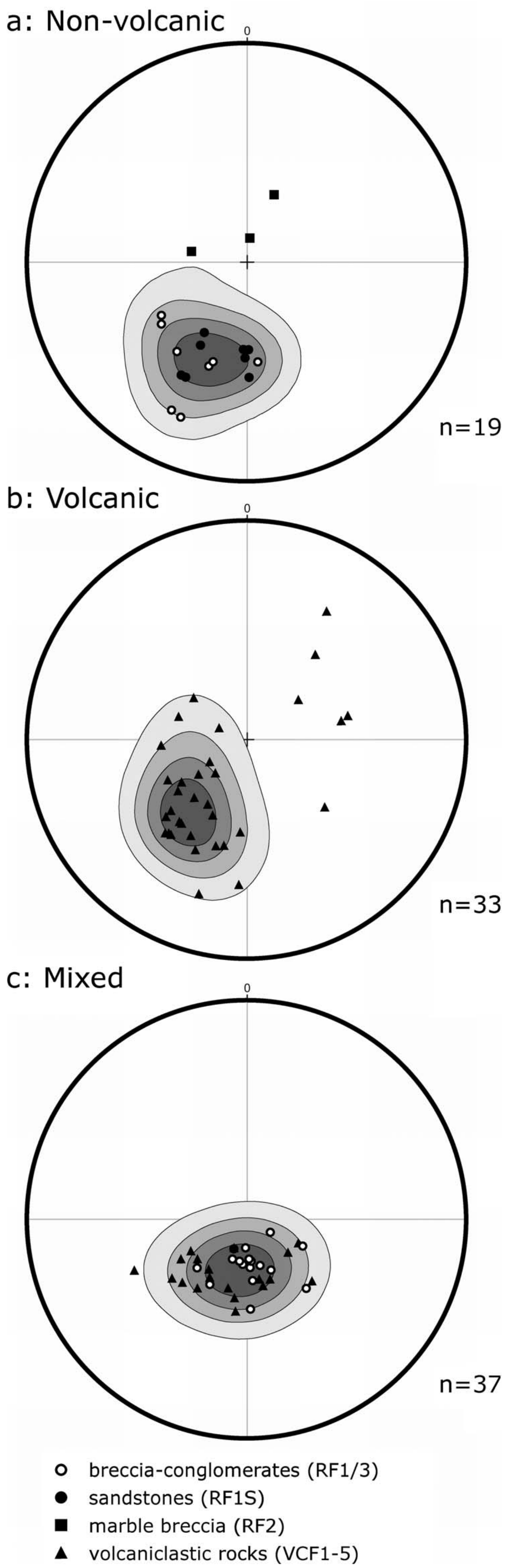

Figure 7. Equal area stereonet projections showing the azimuth and dip of measured beds in the Filipovo–Osenovo section (poles of the respective planes are plotted). The shaded contours represent density distributions from minimum (light grey) to maximum (dark grey); density calculation = cosine sums, cosine exponent = 20, contour intervals = 5, plotted with *Stereo32*. (a) Non-volcanic unit. white circle = breccia-conglomerates (RF1/3), black circle – sandstones (RF1S), square – marble breccia (RF2); n = 19; max. density = 8.86; min. density = 0; mean density = 0.90. (b) Volcanic unit: triangle – volcaniclastic deposits (VCF1–3); n = 33; max. density = 14.00; min. density = 0; mean density = 1.57. (c) Mixed unit: triangle – volcaniclastic deposits (VCF1–5), circle – rudite interbeds (RF1); n = 37; max. density = 21.6; min. density = 0; mean density = 1.76.

angular (RF1) to well-rounded (RF3) clasts, suggests that the transport distance also varied and that material originated from several different source areas. The evolving Mesta Basin, with an emerging footwall ramp along the Mesta Detachment, provided a sufficiently-high gradient for the development of alluvial fan systems, as well as a catchment sink for fluvial systems of the region.

The sheets of massive to crudely stratified breccia-conglomerates were probably deposited by basin margin fans downslope from the footwall along the Mesta Detachment. The original dip of these sediments is not preserved, due to subsequent tilting as a result of displacement along the basin-bounding detachment. However, the dip direction throughout the non-volcanic succession is markedly homogeneous (N–NE) with only slight variations. This observation, combined with the lack of any ubiquitous internal architecture of the rudite sheets (on a bed scale) and clast sizes of up to several metres in diameter, supports the assertions of basin margin fans as the dominant depositional mechanism. The predominant N–S orientation of the confined non-volcanic channel-fill sediments (see RF1 and RF1S) are an exception. Since they indicate sedimentary transport parallel to the N–S-oriented axis of the Mesta Basin, they may be related to partial reworking of the basin margin fans as part of an axial fluvial system (a possible precursor of the present-day river Mesta). However, the volume of sediments contained in axial-oriented channel beds is very low relative to the basin margin fan deposits. Thus, fluvial processes probably played a subordinate role in the depositional environment of the central part of the Mesta Basin compared to the transverse basin margin fans.

The ratio between sediment supply and available accommodation space is a major control on the sedimentary architecture and the stratigraphic succession in a basin (Viseras *et al.* 2003). If a surplus of available sediment relative to the available accommodation space exists in a given time span, the basin is filled up to its lowest-elevation outlet and excess sediment is transported out of the basin. Axial through-drainage develops in such a setting and the sedimentation rate within the basin equals the subsidence rate of the half-graben (Schlische, 1991). If subsidence rate and

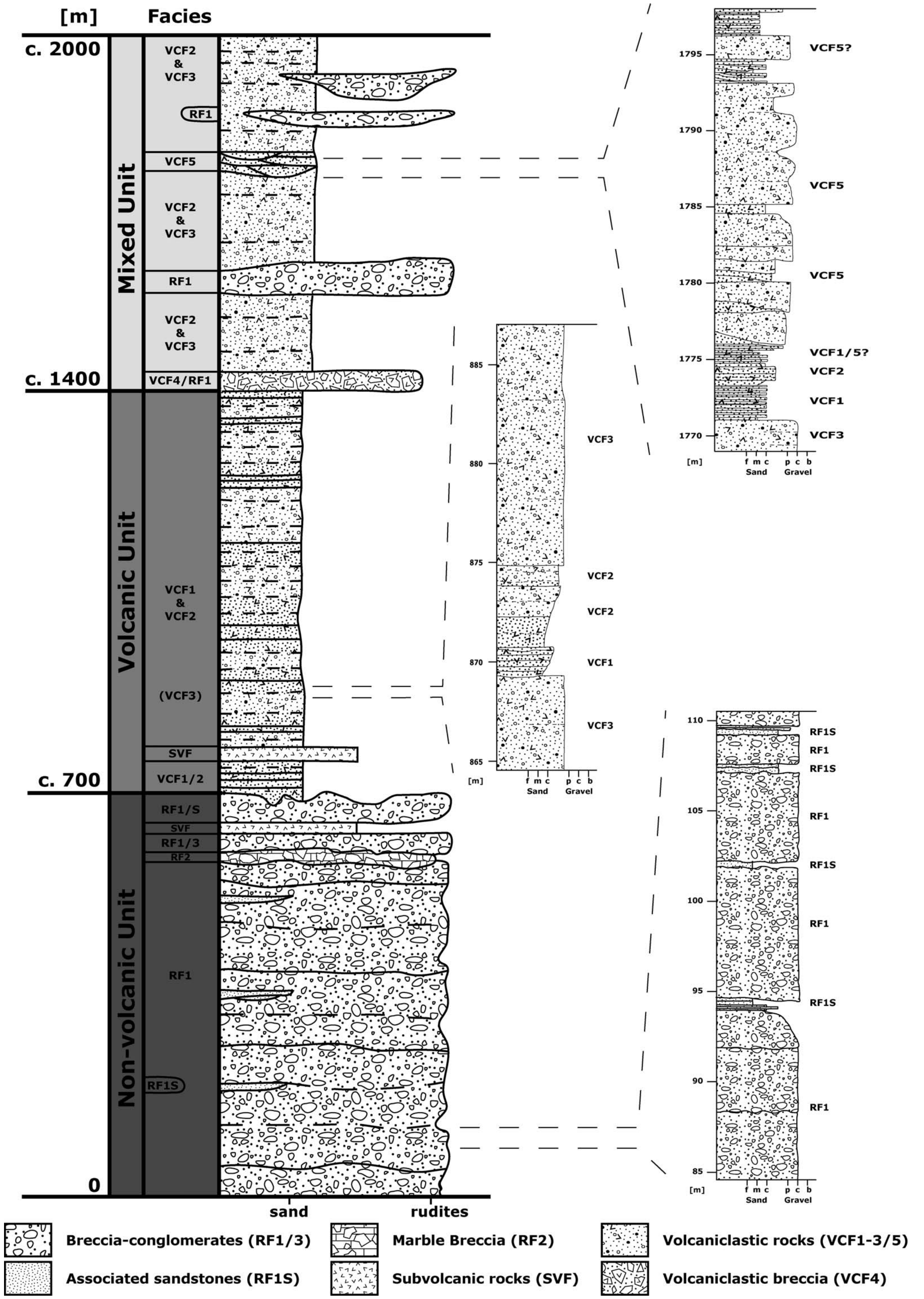

Figure 8. (Left) Schematic sedimentary log of the complete Palaeogene Filipovo–Osenovo section. Bed thickness and geometry are not true to scale but stylized to highlight the key features of the depositional units. (Right) Detailed exemplifying logs (true to scale) for each depositional unit.

https://doi.org/10.1017/S001675680999046X Published online by Cambridge University Press

available accommodation space exceed the sediment supply, only internal sedimentary drainage exists (e.g. lacustrine deposition) and all sediments that enter the basin remain within the basin (Schlische, 1991). Variations in the ratio between sediment supply and accommodation space result in transitions between the end-members of the depositional setting and changes in architectural elements of the facies environment. The nature of the observed sedimentary successions in the Mesta Basin, that is, the lack of any significant volumes of lacustrine sediments within the basin infill (Harkovska, 1983; Burchfiel, Nakov & Tzankov, 2003; present study) and the presence of axial-oriented channel geometries, suggests that axial through-drainage existed throughout the evolution of the basin.

Leeder & Gawthorpe (1987) presented a series of predictive tectono-sedimentary facies models for extensional half-graben basins, which were later expanded upon (e.g. Gawthorpe & Leeder, 2000). The two basic facies models for continental half-graben differ in terms of the major drainage type of the basin: interior drainage or axial through-drainage. As noted above, in terms of drainage, axial through-drainage was dominant in the Mesta Basin. Regardless of the predominant type of drainage in the basin, the fundamental depositional elements contributing to the basin infill are (1) the lateral-transport systems on the footwall and hanging-wall slopes of the half-graben, which were oriented normal to the main basin-bounding faults (here the Mesta Detachment), and (2) the axial sedimentary transport systems parallel to the strike of the main basin-bounding fault (cf. Leeder & Gawthorpe, 1987). The resulting architecture of the basin fill is characteristic of the variable imprints of these two major depositional systems.

The facies model for a continental half-graben with axial through-drainage (Leeder & Gawthorpe, 1987; Gawthorpe & Leeder, 2000) comprises broad alluvial cones on the low-gradient slope of the hanging-wall and alluvial fans downslope from the high-gradient slope of the footwall scarp. The axial fluvial system acts as a pathway for sediment through the basin and may potentially rework the basin margin fans. The lack of any clear and continuous record of such a fluvial system in the Filipovo–Osenovo section, except for several rare and isolated N–S-oriented channels, suggests that the transverse basin margin fans apparently influenced the sedimentary basin infill in the central part of the Mesta Basin to a greater degree than the axial fluvial system. The presence of such relatively large basin margin fans, relative compared to the available accommodation space on the basin plain, may have obstructed the development of any long-term fluvial system in this part of the basin. Combined with the high level of sediment input from the basin margins, this may have resulted in a low preservation potential for the fluvial record of the axial through-drainage system in the central Mesta Basin and a mainly mass flow-dominated depositional environment.

5.b. Volcanic unit

This unit comprises the central part of the succession with a thickness of about 700 m, unconformably overlying the non-volcanic unit. It is characterized by a homogeneous succession of interbedded thin- to thick-bedded and massive volcaniclastic deposits. The complete absence of any primary non-volcanic layers is remarkable. The bed contacts are sharp, erosive or gradual. The bed geometry is parallel or lenticular. Most of the beds are discontinuous over a scale of tens to hundreds of metres. The thickness of a bed apparently correlates with the lateral continuity; increased thickness corresponds to a greater lateral extent. The dip direction of the volcaniclastic beds in the volcanic unit are predominantly NE (Fig. 7b), although other dip directions also occur. These fluctuations may be related to different source areas for the volcanogenic material or to the existence of an uneven basin topography. Pre-existing basin lows with variable slope orientations may also have acted as a catchment area for the volcanic material and thus influenced the resultant dip directions of the deposits. The dip angles vary from 63 to 11° (Fig. 7b).

The basal contact with the underlying non-volcanic unit is irregular, with locally steep-angled contacts, and probably represents an angular unconformity associated with synsedimentary faulting. This suggests that the basin topography was fairly uneven at the time of the deposition of the volcanic unit and possibly the result of prior erosion of the non-volcanic breccia-conglomerates and the development of incised valleys or channels during a phase of reduced subsidence, low sediment supply or a short pulse of uplift in the region. Compartmentalization of the basin due to intrabasinal faults could also be responsible. In either case, an uneven basin floor topography with basin lows between highs of remnant non-volcanic deposits would have existed. These topographic lows were subsequently filled with volcanic material.

As noted in Section 4.b, a variety of pyroclastic density currents characterize this unit. Their genesis was related to the collapse of explosive eruption columns. Particle concentration, size distribution and the density of the particles (cf. Choux, Druitt & Thomas, 2004), as well as the water content, determined the type of flow. The volcanic unit marks the first occurrence of volcaniclastic material within the Filipovo–Osenovo section, and therefore probably represents the onset of explosive volcanic activity within the basin. The volcanic material was probably derived from the nearby Kremen caldera, about 10 km to the south of the Filipovo–Osenovo area, or from other volcanic centres in the southern part of the Mesta Basin (Harkovska *et al.* 1998).

The facies variations in the volcaniclastic rocks of this unit may be related either to different eruptions, to eruption pulses of variable strength or to sequential partial collapse of the same eruption column. Another possible explanation may be related to the variable distances to the volcanic centres with the thinner volcaniclastic beds representing a distal facies, while the thicker beds were deposited in a more proximal facies.

The absence of any primary non-volcanic or clearly reworked volcaniclastic sediments in the central part of the Filipovo–Osenovo succession indicates that the non-volcanic input from the basin margin fans was negligible during the deposition of this unit and that this depositional setting probably covers a fairly short time period. Large volumes of tephra and pyroclastic deposits can be generated in days to weeks (e.g. Jenkins, Magill & McAneney, 2007; Mason, Pyle & Oppenheimer, 2004). Thus, the volcanic unit in the Filipovo–Osenovo may represent the pyroclastic deposits of several pronounced volcanic eruptions occurring over a relatively short period of time during which no basin margin fan deposition occurred.

5.c. Mixed unit

The mixed unit forms the top of the Palaeogene sedimentary succession with a thickness of about 600 m and comprises both volcaniclastic deposits, similar to those of the prior unit, interbedded with non-volcanic rudites (up to tens of metres thick) and redeposited volcaniclastic rocks. The internal structure of the primary volcaniclastic rocks is characterized by fewer thin- to medium-bedded (VCF1) and more thick-bedded to massive volcaniclastic rocks (VCF2–3). Reworked volcaniclastic sediments can be identified by the abundance of altered volcanic clasts and sedimentary structures, which are typical for a fluvial facies. The secondary volcaniclastic sediments often occur in the form of lenticular sedimentary bodies and may represent the fill of fluvial channels.

The contact with the underlying volcanic unit is marked by an unconformity. Here primary fine- to thick-bedded volcaniclastic rocks of the volcanic unit (VCF1–2) are directly overlain by a secondary volcaniclastic breccia (VCF4). Towards the top of the succession, the mixed unit is overlain by Neogene-age sandy conglomerates.

The dip direction of the strata is uniform NW to NE. The dip angles vary between 35 and 10° for the volcaniclastic rocks and between 47 and 20° for the breccia-conglomerates (Fig. 7c). The azimuth distribution shows a slightly two-fold division: the non-volcanic breccia-conglomerate interbeds dip more frequently to the NE, while the volcaniclastic beds dip more often to the NW. These variations in both azimuth and dip may have resulted from different depositional processes and/or source areas.

The interbedded breccia-conglomerates are similar in appearance to the clast-supported breccia-conglomerates of the basal non-volcanic unit (RF1), and thus, similar depositional processes (sedimentary gravity flows) can be assumed. The breccia-conglomerates occur, with the exception of one unit (up to tens of metres thick), as isolated beds. Interestingly, the beds contain no significant volcaniclastic material, suggesting that during sedimentary transport and deposition, no volcanic material was eroded and entrained. Therefore, one-off events, such as mass flows derived from basin margin fans, are much more likely to be the determining depositional process.

Another difference with the underlying volcanic unit is the occurrence of reworked volcaniclastic material in lenticular interbeds. Altered volcanic clasts and crystals (especially plagioclase), tectonically stressed quartz and fluvial sedimentary structures indicate that the primary volcaniclastic deposits were partially eroded and subsequently reworked in fluvial systems in the basin.

The depositional setting for the mixed unit was most likely characterized by occasional mass flows originating from the basin margins into a setting dominated by periods of explosive volcanic activity with the deposition of pyroclastic sediments. During longer periods of no, or waning, eruptions, partial reworking of the exposed volcaniclastic deposits took place and alluvial basin margin fans were active. The non-volcanic fan deposits were subsequently buried when a new eruption cycle commenced.

6. Basin evolution

Analysis of the Filipovo–Osenovo section, together with supporting data from the entire Palaeogene succession, suggests that there were three depositional stages for the central part of the Mesta Basin. The two main factors controlling the depositional framework for the basin were (1) tectonic activity along the eastern margin detachment and resultant slopes due to hangingwall downtilting and footwall uplift and (2) the onset and intensity of volcanic activity within the basin. The facies variations can thus be related to the changing effects, influences and emphasis of alluvial and volcanic processes. Each depositional stage corresponds to one of the previously discussed depositional units (see Section 5). We also suggest depositional ages for each stage. These ages are based on a very limited amount of data (namely, palynological data of Ivanov & Chernyavska, 1972; geochronological data of Pecskay, Harkovska & Hadjiev, 2000; and stratigraphic correlations by Zagorchev, 1998) and much more detailed work is required in order to constrain fully the depositional timeframes. However, the presented ages are the current best estimates and as such constitute an important base for discussion.

Basin evolution commenced with a period of rapid extension and the development of the eastern margin

https://doi.org/10.1017/S001675680999046X Published online by Cambridge University Press

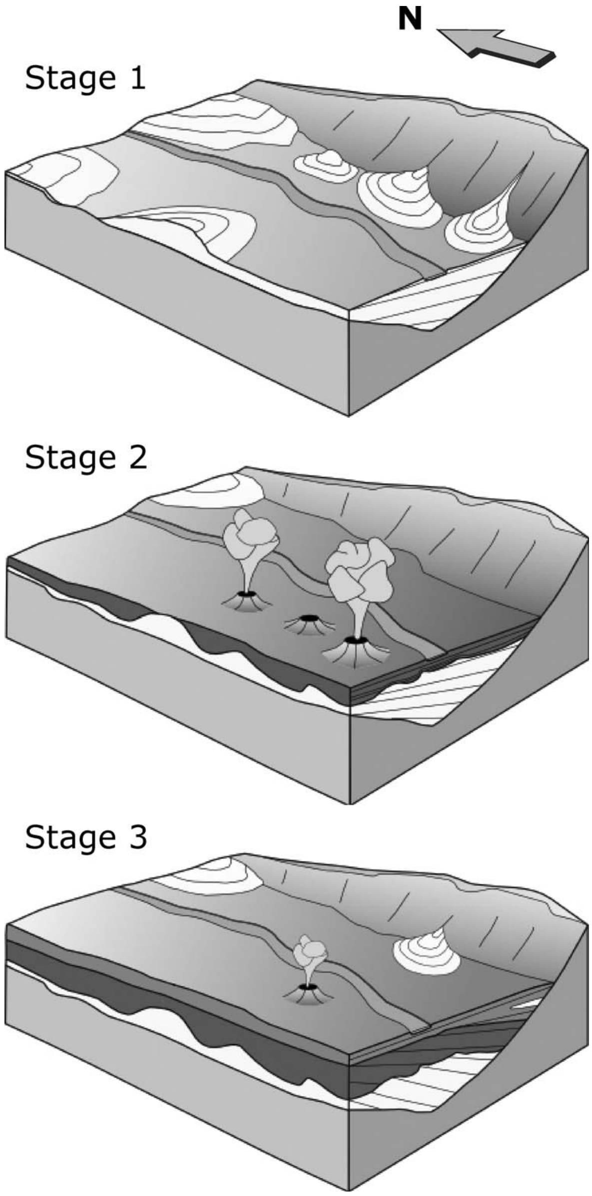

Figure 9. Three simplified block diagrams illustrating stages in the evolution of the central part of the Mesta Basin. Each stage corresponds to one of the described depositional units in the text.

detachment (Stage 1, Fig. 9). This resulted in the production of accommodation space in a N–S-oriented trough-shaped basin. The resultant sink was probably composed of an emerging footwall ramp along the eastern margin, a gentler slope on the western hanging-wall side of the basin, several alluvial basin margin fans prograding downslope from the eastern fault scarp and a N–S axial sediment drainage system with active fluvial processes. The initial depositional setting, dominated by the deposition of breccia-conglomerates and sandstones, comprised an alluvial environment in an axial through-drainage half-graben with associated basin margin fans. The basin margins were the main sources of the various sedimentary gravity flows transporting sediment into the basin. The axial fluvial system transported additional material from surrounding basement highs as well as reworking the more distal parts of the basin margin fans.

Based on the fact that the basal breccia-conglomerates of the Filipovo–Osenovo section unconformably overlie basement, similar depositional ages to the Late Eocene Gradinishka Formation (Priabonian; Ivanov & Chernyavska, 1972; Zagorchev, 1998) can be assumed. The other time constraint for this depositional unit was the onset of volcanic activity within the Mesta Basin. The basal non-volcanic depositional unit does not contain any volcanic material and is directly unconformably overlain by primary volcaniclastic deposits. Pecskay, Harkovska & Hadjiev (2000) dated the onset of explosive volcanic activity within the Mesta Basin as Rupelian (33 Ma). Given these limited age constraints, the time interval for this depositional stage can be roughly estimated as Late Eocene, that is, 38 to 33 Ma.

The second stage of basin evolution was characterized by the homogeneous volcaniclastic succession and thus coincides with the onset of volcanic activity (Stage 2, Fig. 9). Volcanic centres developed in the region in response to continued crustal thinning. The irregular contact between the underlying non-volcanic breccia-conglomerates and the basal part of the volcaniclastic succession suggests that there was a significant amount of relief, which was then filled with volcanogenic material during an intense phase of explosive volcanic activity. The absence of any interbedded non-volcanic alluvial sediments in this part of the succession indicates rapid infilling, possibly during several eruption cycles over a period of days to months (see Section 5.b). The volcanic material was probably derived from the nearby volcanic centres at Kremen and Banichan and was deposited by pyroclastic flows and surges, although occasional tephra fall-out deposits have also been noted.

Pecskay, Harkovska & Hadjiev (2000) suggested a Rupelian age (33–31 Ma) for the onset of magmatic activity in the Kremen–Gostun–Dobrinishte Zone. Therefore, the time interval for the second depositional stage can be estimated as extending over a period of days to months at sometime in the Early Oligocene between 33 to 31 Ma.

The third stage was characterized by alternating volcaniclastic and alluvial depositional cycles, produced as the result of waning volcanic activity (Stage 3, Fig. 9). Periods with little or no volcanic activity provided time windows for the deposition of alluvial sediments. The resultant sedimentary units were subsequently buried by volcanic deposits during renewed periods of explosive activity. Due to the longer timeframe of this stage, volcaniclastic sediments were also exposed on the basin floor and were subject to partial reworking, as evidenced by the occurrence of reworked and redeposited volcaniclastic material in fluvial channels. Probably contemporaneously with the final eruptive volcanic phases, subvolcanic bodies were intruded in the lower part of the succession. The timeframe for the third stage is more difficult to constrain. The youngest volcanic activity within the Mesta Basin was dated as Late Oligocene (28 Ma; Pecskay, Harkovska & Hadjiev, 2000). Thus, the time interval for this depositional unit can be estimated as Early to Late Oligocene between 31 to 28 Ma. Subsequent to this stage, volcanic activity apparently ceased within the basin and the Palaeogene succession was partly eroded and unconformably overlain by Neogene alluvial systems.

7. Conclusions

The Mesta Basin in SW Bulgaria is one of a series of continental extensional basins in the Rhodope Zone that developed as a result of Late Eocene extension in the Aegean area. The basin is a half-graben with axial through-drainage and is bounded on the eastern margin by the Mesta Detachment. Basin infill comprises a more than 2500 m thick succession of Palaeogene interbedded alluvial and volcaniclastic rocks and subvolcanic intrusions.

The best indicators for stratigraphic relationships between the various units are the superpositional relationships, which are clearly observed in several continuous successions throughout the basin. These successions are also mostly characterized by the progressive lessening of dip towards the top of the succession. Detailed analysis of these transverse sections may allow the correlation of depositional units based on a combination of structural data (degree of rotation), lithology and relationships between volcanic and non-volcanic units.

The continuous 2000 m thick sedimentary succession between the villages of Filipovo and Osenovo is a representative key section of the basin fill in the central part of the Mesta Basin. The section comprises three main facies associations (non-volcanic breccia-conglomerates and associated sandstones, volcaniclastic deposits and subvolcanic rocks) that can be grouped into three depositional units (non-volcanic, volcanic, mixed), based on lithofacies associations and facies architecture. The overall depositional environment in the basin was influenced by the interaction between interdigitating basin margin fans and a fluvial through-drainage system, compartmentalization by intrabasinal faults, explosive volcanic activity and the relative distance to the volcanic centres. Displacement along the Mesta Detachment resulted in synsedimentary rotation and exerted a fundamental control upon facies distribution within the basin.

The evolution of the Mesta Basin commenced with a period of rapid extension and the resultant creation of accommodation space, accompanied by alluvial sedimentation (Stage I). The onset of volcanic activity in response to crustal thinning coincided with the infilling of the basin with volcanogenic material (Stage II). Subsequent waning of volcanic activity coincided with the re-establishment of alluvial conditions and alternating alluvial and volcaniclastic depositional cycles (Stage III). The Palaeogene sediments were subsequently buried under Neogene alluvial sediments and partly eroded by the incision of the present-day Mesta River.

Acknowledgements. The authors would like to thank Rob Westaway and two anonymous reviewers for their helpful comments that improved the manuscript considerably. This work was supported by a Deutsche Forschungsgemeinschaft grant to T. McCann (DFG MC 10/9-1).

References

BLAIR, T. C. & MCPHERSON, J. G. 1992. The Trollheim alluvial fan and facies model revisited. *Geological Society of America Bulletin* **104**, 762–9.

BLAIR, T. C. & MCPHERSON, J. G. 1994. Alluvial fans and their natural distinction from rivers based on morphology, hydraulic processes, sedimentary processes, and facies assemblages. *Journal of Sedimentary Research* **64**(3), 450–89.

BONEV, N., BURG, J. P. & IVANOV, Z. 2006. Mesozoic–Tertiary structural evolution of an extensional gneiss dome – the Kesebir–Kardamos dome, eastern Rhodope (Bulgaria–Greece). *International Journal of Earth Sciences* **95**(2), 318–40.

BURCHFIEL, B. C., KING, R. W., NAKOV, R., TZANKOV, T., DUMURDZANOV, N., SERAFIMOVSKI, T., TODOSOV, A. & NURCE, B. 2008. Patterns of Cenozoic Extensional Tectonism in the South Balkan Extensional System. In *Earthquake Monitoring and Seismic Hazard Mitigation in Balkan Countries* (ed. E. S. Husebye), pp. 3–18. Springer Science + Business Media B.V.

BURCHFIEL, B. C., NAKOV, R. & TZANKOV, T. 2003. Evidence from the Mesta halfgraben, SW Bulgaria, for the Late Eocene beginning of Aegean extension in the Central Balkan Peninsula. *Tectonophysics* **375**, 61–76.

BURCHFIEL, B. C., NAKOV, R., TZANKOV, T. & ROYDEN, L. H. 2000. Cenozoic extension in Bulgaria and northern Greece: the northern part of the Aegean extensional regime. In *Tectonics and Magmatism in Turkey and the Surrounding Area* (eds E. Bozkurt, J. A. Winchester & J. D. A. Piper), pp. 325–52. Geological Society of London, Special Publication no. 173.

BURGISSER, A. & BERGANTZ, G. W. 2002. Reconciling pyroclastic flow and surge: the multiphase physics of pyroclastic density currents. *Earth and Planetary Science Letters* **202**, 405–18.

CAS, R. A. F. & WRIGHT, J. V. 1987. *Volcanic Successions, Modern and Ancient*. London: Allen & Unwin Ltd, 528 pp.

CHOUX, C., DRUITT, T. & THOMAS, N. 2004. Stratification and particle segregation in flowing polydisperse suspensions, with applications to the transport and sedimentation of pyroclastic density currents. *Journal of Volcanology and Geothermal Research* **138**, 223–41.

COLLINSON, J., MOUNTNEY, N. & THOMPSON, D. 2006. Depositional structures in gravels, conglomerates and breccias. In *Sedimentary Structures* (eds J. Collinson, N. Mountney & D. Thompson), pp. 138–62. Terra Publishing.

COUSSOT, P. & MEUNIER, M. 1996. Recognition, classification and mechanical description of debris flows. *Earth-Science Reviews* **40**, 209–27.

DHONT, D., YANEV, Y., BARDINTZEFF, J. M. & CHOROWICZ, J. 2008. Evolution and relationships between volcanism and tectonics in the central-eastern part of the Oligocene Borovitsa caldera (Eastern Rhodopes, Bulgaria).

Journal of Volcanology and Geothermal Research **171**, 269–86.
DINTER, D. A. 1998. Late Cenozoic extension of the Alpine collisional orogen, northeastern Greece: Origin of the north Aegean basin. *Geological Society of America Bulletin* **110**(9), 1208–26.
FELIX, M. & PEAKALL, J. 2006. Transformation of debris flows into turbidity currents: mechanisms inferred from laboratory experiments. *Sedimentology* **53**, 107–23.
FISHER, R. V. & SCHMINCKE, H. U. 1984. *Pyroclastic Rocks*. Berlin: Springer Verlag, 472 pp.
GAWTHORPE, R. L. & LEEDER, M. R. 2000. Tectono-sedimentary evolution of active extensional basins. *Basin Research* **12**, 195–218.
HARKOVSKA, A. 1983. Spatial and temporal relations between volcanic activity and sedimentation in the stratified Paleogene from the central parts of Mesta Graben (SW Bulgaria). *Geologica Balcanica* **13**, 3–30.
HARKOVSKA, A., MARCHEV, P., MACHEV, P. & PECSKAY, Z. 1998. Paleogene magmatism in the Central Rhodope area, Bulgaria – A review and new data. *Acta Vulcanologica* **10**(2), 199–216.
IVANOV, R. & CHERNYAVSKA, S. 1972. Geological, petrographical and palynological data on the age of the Paleogene volcanic activity in Western Bulgaria: 3. The Paleogene of Mesta (in Bulgarian with English summary). *Bulletin of the Geological Institute, Series Stratigraphy and Lithology* **XXI**, 85–100.
IVANOVA, R. 2005. Volcanology and petrology of acid volcanic rocks from the Paleogene Sheinovets caldera, Eastern Rhodopes. *Geochemistry, Mineralogy and Petrology* **42**, 23–45.
JENKINS, S. F., MAGILL, C. R. & MCANENEY, K. J. 2007. Multi-stage volcanic events: A statistical investigation. *Journal of Volcanology and Geothermal Research* **161**, 275–88.
LEEDER, M. R. & GAWTHORPE, R. L. 1987. Sedimentary models for extensional tiltblock/half-graben basins. In *Continental Extensional Tectonics* (eds M. P. Coward, J. F. Dewey & P. L. Hancock), pp. 139–52. Geological Society of London, Special Publication no. 28.
LUBE, G., CRONIN, S. J., PLATZ, T., FREUNDT, A., PROCTER, J. N., HENDERSON, C. & SHERIDAN, M. F. 2006. Flow and deposition of pyroclastic granular flows: A type example from the 1975 Ngauruhoe eruption, New Zealand. *Journal of Volcanology and Geothermal Research* **161**, 165–86.
MALET, J. P., LAIGLE, D., REMAITRE, A. & MAQUAIRE, O. 2005. Triggering conditions and mobility of debris flows associated to complex earthflows. *Geomorphology* **66**, 215–35.
MASON, B. G., PYLE, D. M. & OPPENHEIMER, C. 2004. The size and frequency of the largest explosive eruptions on Earth. *Bulletin of Volcanology* **66**, 735–48.
MCPHIE, J., DOYLE, M. & ALLEN, R. L. 1993. *Volcanic textures: a guide to the interpretation of texture in volcanic rocks*. CODES SRC, University of Tasmania, 198 pp.
MULDER, T. & ALEXANDER, J. 2001. The physical character of subaqueous sedimentary density flows and their deposits. *Sedimentology* **48**, 269–99.
NEMEC, W. & STEEL, R. J. 1984. Alluvial and coastal conglomerates: their significant features and some comments on gravelly mass-flow deposits. In *Sedimentology of Gravels and Conglomerates* (eds E. H. Koster & R. J. Steel), pp. 1–31. Canadian Society of Petroleum Geologists, Memoir no. 10.
PECSKAY, Z., HARKOVSKA, A. & HADJIEV, A. 2000. K–Ar dating of the Mesta volcanics (SW Bulgaria). *Geologica Balcanica* **30**(1–2), 3–11.
RICOU, L. E., BURG, J. P., GODFRIAUX, I. & IVANOV, Z. 1998. Rhodope and Vardar: the metamorphic and the olistromic paired belts related to Cretaceous subduction under Europe. *Geodinamica Acta* **11**(6), 285–309.
RICOU, L. E., BURG, J. P., GODFRIAUX, I. & IVANOV, Z. 2000. Reply to Ivan Zagorchev's comment 'Rhodope facts and Tethys self-delusions'. *Geodinamica Acta* **13**(1), 61–3.
ROCHE, O., GILBERTSON, M. A., PHILLIPS, J. C. & SPARKS, R. S. J. 2005. Inviscid behaviour of fines-rich pyroclastic flows inferred from experiments on gas-particle mixtures. *Earth and Planetary Science Letters* **240**, 401–14.
SALVADOR, A. 1994. *International Stratigraphic Guide: A Guide to Stratigraphic Classification, Terminology, and Procedure*, 2nd ed. International Union of Geological Sciences and Geological Society of America, 214 pp.
SCHLISCHE, R. W. 1991. Half-graben basin filling models: new constraints on continental extensional basin development. *Basin Research* **3**, 123–41.
SPARKS, R. S. J., BURSIK, M. I., CAREY, S. N., GILBERT, J. S., GLAZE, L. S., SIGURDSSON, H. & WOODS, A. W. 1997. *Volcanic plumes*. John Wiley & Sons Ltd, 574 pp.
TUECKMANTEL, C., SCHMIDT, S., NEISEN, M., GEORGIEV, N., NAGEL, T. J. & FROITZHEIM, N. 2008. The Rila-Pastra Normal Fault and multi-stage extensional unroofing in the Rila Mountains (SW Bulgaria). *Swiss Journal of Geosciences* **101**, 295–310.
VISERAS, C., CALVACHE, M. L., SORIA, J. M. & FERNANDEZ, J. 2003. Differential features of alluvial fans controlled by tectonic or eustatic accommodation space. Examples from the Betic Cordillera, Spain. *Geomorphology* **50**, 181–202.
WALTHAM, D. 2004. Flow transformations in particulate gravity currents. *Journal of Sedimentary Research* **74**, 129–34.
WESTAWAY, R. 2006. Late Cenozoic extension in SW Bulgaria: a synthesis. In *Tectonic development of the Eastern Mediterranean Region* (eds A. H. F. Robertson & D. Mountrakis), pp. 557–90. Geological Society of London, Special Publication no. 260.
ZAGORCHEV, T. 1998. Pre-Priabonian Paleogene formations in southwestern Bulgaria and northern Greece: stratigraphy and tectonic implications. *Geological Magazine* **135**, 101–19.
ZAGORCHEV, T. 2000. Comment: Rhodope facts and Tethys self-delusions. *Geodinamica Acta* **13**(4), 55–9.